Study of growth and electrical conductivity of ultrathin magnesium films on bismuth-passivated Si(111) surface

© D.A. Tsukanov[1,2], S.G. Azatyan[1], N.V. Denisov[1], M.V. Ryzhkova[1]

[1] Institute of Automation and Control Processes, Far Eastern Branch of Russian Academy of Sciences,
690041 Vladivostok, Russia
[2] Far Eastern Federal University,
690090 Vladivostok, Russia

E-mail: tsukanov@iacp.dvo.ru

Received June 23, 2025
Revised August 14, 2025
Accepted August 14, 2025

The results of the study of the crystal structure, morphology and electrical resistance of Si(111) substrates after magnesium deposition on pre-formed surface reconstructions of Si(111)$\sqrt{3}\times\sqrt{3}$-Bi are presented. Low-energy electron diffraction and scanning tunneling microscopy were used to study changes in the crystal lattice structure and surface morphology, and the four-probe method was used to measure the electrical resistance of the substrates *in situ*. The effect of the concentration of adsorbed magnesium atoms on the structural and electrical properties of the films is considered. The role of surface reconstructions as a buffer layer for subsequent growth of ultrathin magnesium films is shown.

Keywords: adsorption, surface reconstruction, electrical resistance, low-energy electron diffraction, four-point probe method.

DOI: 10.61011/SC.2025.06.62059.7739

1. Introduction

In recent decades, reconstructions induced by metal atoms on the single crystal surface of the Si(111) substrate have continued to attract wide attention due to the wide variety of their structural and electronic properties observed in these systems. But from another point of view, it is obvious that the reconstructed surface itself is a good platform for the subsequent growth of ultrathin films, low-dimensional materials, and nanostructures [1–5], when the growth mechanisms of such structures and films may depend on which surface reconstruction was previously formed on the substrate.

One of the specific systems that has been the object of increased interest in recent years is the surface reconstruction of Si(111)$\sqrt{3}\times\sqrt{3}$-Bi. As is well known, this structure is represented by two reconstructions with periodicity $\sqrt{3}\times\sqrt{3}$ [6], such as Si(111)-$\alpha\sqrt{3}\times\sqrt{3}$-Bi (hereinafter $\alpha\sqrt{3}$-Bi) with 1/3 monolayer (ML) of bismuth coating (bismuth adatoms occupy single T4 positions on the volume-like surface Si(111) [7]) and Si(111)-$\beta\sqrt{3}\times\sqrt{3}$-Bi (hereinafter $\beta\sqrt{3}$-Bi) with 1 ML of bismuth, where the bismuth atoms are organized into trimers near the T4 position in accordance with the „milk stool“ model [8,9]). According to the research results obtained using scanning tunneling microscopy (STM), the surface of $\alpha\sqrt{3}$-Bi, in contrast to $\beta\sqrt{3}$-Bi, contains a high density of defects due to the substitution of bismuth atoms with silicon atoms from the substrate [10] and it has unsaturated dangling bonds, which makes this surface a suitable site for the formation of various nanostructures and ultrathin films by adsorption of foreign atoms on the surface. For example, it was shown that deposition of ~ 1.2 ML of aluminum onto the surface of $\alpha\sqrt{3}$-Bi at room temperature leads to the formation of a three-component surface phase of Si(111)2×2-(Bi,Al) [11]. In the case of silver deposition on the surface of $\alpha\sqrt{3}$-Bi, quasi-ordered metastable structures (Bi,Ag)/Si(111) [12] are formed. Sputtering of 1/3 ML of lead onto the surface of $\alpha\sqrt{3}$-Bi followed by heating of the substrate at 550 °C for 3 min leads to the formation of a reconstruction of Si(111)$2\sqrt{3}\times 2\sqrt{3}$-(Pb,Bi), in the electronic structure of which the Rashba splitting is observed [13]. Despite the fact that the surface phase of $\alpha\sqrt{3}$-Bi has interesting prospects for the growth of various structures obtained by metal adsorption, there are still no systematic studies devoted to studying the interaction of adsorbed atoms with this surface.

The influence of Si(111)$\sqrt{3}\times\sqrt{3}$-Bi surface structures on the subsequent growth of ultrathin magnesium films was experimentally studied in this paper. Two reconstructions induced by bismuth atoms were selected for evaluation of the effect of the initial surface reconstruction on the behavior of the second metal: $\alpha\sqrt{3}$-Bi and $\beta\sqrt{3}$-Bi, which differ from each other in lattice structure and atomic density. It was already reported in early papers [10,14], that these surfaces significantly affect the processes of adsorption and the growth mechanisms of adsorbed materials. For example, it is known that the growth of gold films on the surface of α-$\sqrt{3}$-Bi follows the Stransky–Krastanov mechanism, while the Vollmer–Weber growth mechanism is observed on the surface of β-$\sqrt{3}$-Bi [10]. It was shown in Ref. [14] that hydrogen adsorption on the surface of Si(111)$\sqrt{3}\times\sqrt{3}$-Bi occurs mainly in regions with the phase α-$\sqrt{3}$-Bi, rather

than on $\beta\sqrt{3}$-Bi, because the bismuth trimers, which make up the $\beta\sqrt{3}$-Bi phase, prevent the interaction of hydrogen atoms with silicon.

Low-energy electron diffraction (LEED) and scanning tunneling microscopy (STM) were used in this work to study this issue. Since it is well known that the electrical conductivity of silicon substrates critically depends on changes in the atomic structure of the surface and surface morphology [15], we measured the surface electrical conductivity of films grown on reconstructed Bi/Si(111) surfaces using a four-probe the method.

2. Experimental conditions

The experiments were carried out in two separate ultrahigh vacuum (UHV) chambers with a base pressure in the range of 10^{-10} Torr. The first UHV chamber provided with STM and LEED methods was used to study the crystal structure and morphology of Si(111) substrates with a reconstructed surface before and after the adsorption of the material, magnesium or bismuth. In the second UHV chamber, provided with a LEED and an attachment for measuring the surface conductivity of samples using the four-probe *in situ* method, surface reconstructions were formed and bismuth or magnesium were sputtered under the same conditions as in the first chamber, and electrical measurements were also performed. The measuring four-probe head is located on a retractable manipulator and contains electrochemically pointed probes made of tungsten wire (0.7 mm thick) pressed against the surface by separate springs. The probes are located in the corners of the square with sides 0.6×0.6 mm. Low-noise precision DC/AC current source Keithley 6221 and nanovoltmeter Keithley 2182A were used as meters, which in the δ-system mode ensure a reliable and reproducible characterization of the materials under study by separating current and voltage measurements. All conductivity measurements were carried out under stable conditions at room temperature. If high-temperature heating of the substrate was required, electrical measurements were carried out at least one hour after the annealing procedure. The results of each measurement were expressed in Ohm/square units (surface resistance) and represented the average value of the electrical resistance for different pairs of probes and current directions.

The substrates were cut from standard Si(111) wafers doped with phosphorus (n-type), with a resistivity of $300-1700$ Ohms $\cdot$ cm. The size of the samples was $12\times2\times0.45$ mm for the STM study and $15\times5\times0.45$ mm for electrical measurements. The surface of the samples was cleaned first by washing and cleaning in organic solvents, drying, and then the samples were placed in the UHV chamber, where the atomically pure surface is Si(111)7×7 was prepared by flashing to 1250 °C after preliminary degassing of the sample by resistive heating at 600 °C for several hours. The temperature of the samples was monitored by an infrared pyrometer, and at temperatures below 300 °C temperature measurements were carried out using a thermocouple.

Bismuth and magnesium were sprayed onto the surface of the substrate from sources such as Knudsen cells, which were degassed tantalum tubes filled with the appropriate material. The amount of deposited material was determined in monolayers (ML), 1 ML corresponds to the surface concentration of atoms equal to $7.83\cdot10^{12}$ atoms/cm^2 for Si(111). The deposition rate of bismuth was calibrated by forming a reconstruction of Si(111)$\sqrt{3}\times\sqrt{3}$-Bi, in which the phases $\alpha\sqrt{3}$-Bi and $\beta\sqrt{3}$-Bi with 1/3 ML and 1 ML coatings bismuth, respectively, differed from each other using LEED observations (details are presented in Ref. [6]). The deposition rate of magnesium was calibrated using observations of the Si(111) surface reconstruction3×1-Mg formed after spraying 1/3 ML of magnesium onto the surface of Si(111)7×7 [16]. All the structures described in this paper were created by precipitation of magnesium on the surface of $\alpha\sqrt{3}$-Bi or $\beta\sqrt{3}$-Bi, or a surface where the phases $\alpha\sqrt{3}$-Bi and $\beta\sqrt{3}$-Bi are present simultaneously (mixed surface $\alpha+\beta\sqrt{3}$-Bi).

3. Experimental results and discussion

Two reconstructions of the Si(111)$\sqrt{3}\times\sqrt{3}$-Bi surface were used to demonstrate the effect of the substrate surface on the growth modes and electrical conductivity of the grown magnesium layers: $\alpha\sqrt{3}$-Bi and $\beta\sqrt{3}$-Bi. The $\beta\sqrt{3}$-Bi phase was prepared by precipitation of 1 ML of bismuth onto the surface of Si(111)7×7, kept at room temperature, followed by annealing at $450-500$ °C, while the surface of $\alpha\sqrt{3}$-Bi (see LEED image in Figure 1, *a*) was prepared by annealing of a sample with the reconstruction of $\beta\sqrt{3}$-Bi surface at ~600 °C to cause desorption of excess Bi atoms. $\alpha\sqrt{3}$-Bi and $\beta\sqrt{3}$-Bi structures can be confidently distinguished in the LEED images by observing the intensity of reflexes at the energy of the primary beam ~80 eV [6].

According to the observation of diffraction patterns of the surface, deposition of >0.6 ML of magnesium onto the surface of $\alpha\sqrt{3}$-Bi at room temperature leads to the formation of 2×2 superstructure (Figure 1, *b*). After further deposition of magnesium (approximately with a total coating of more than 2 ML of magnesium), the structure of 2×2 disappears completely and a symmetrical LEED pattern is observed (Figure 1, *c*), which indicates an average pattern composed of two regular structures: Si(111)1×1 substrate and *hcp*-structure of Mg(0001). Comparing the distances between the diffraction spots of the main reflections 1×1 of the Si(111) surface and the reflexes of the second*hcp*-structure, it is possible to obtain a lattice constant in the film plane equal to 3.24 Å, which is close to 3.21 Å for the lattice of bulk magnesium Mg(0001) [17]. „2×2“ reflexes are observed in the LEED pattern after precipitation from 2.7 to 8 ML of magnesium, rotated by 15° relative to the directions Si(111), along with basic reflexes from Mg(0001) (Figure 1, *d*). It should be noted that these

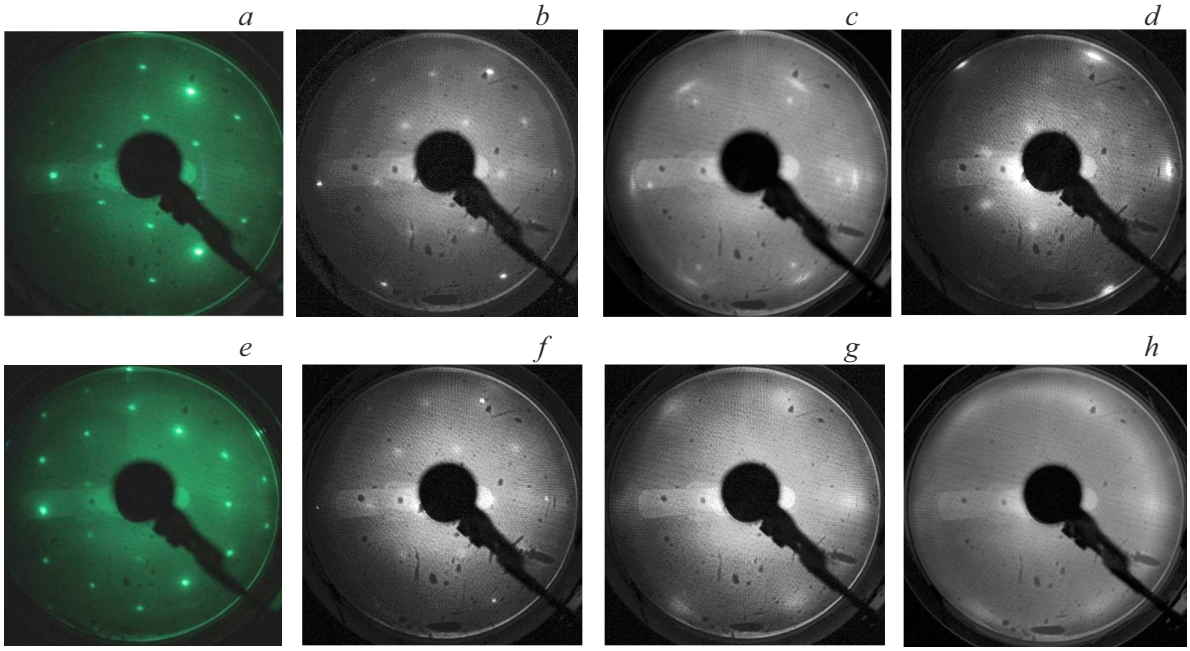

Figure 1. LEED patterns recorded for the surface of $\alpha\sqrt{3}$-Bi (75 eV) before (*a*) and after precipitation of magnesium at room temperature: *b* — 1.2 ML (40 eV), *c* — 2 ML (70 eV) and *d* — 8 ML (40 eV). $\beta\sqrt{3}$-Bi surface before (*e*) and after deposition of 1.2 ML (*f*) and 8 ML (*g*) of magnesium. *h* — Si(111)7×7 surface after precipitation of 8 ML of magnesium at room temperature.

reflexes differ from those of the surface reconstruction of Si(111)2×2-(Bi,Mg) both in terms of rotation angle and in terms of location in the diffraction pattern.

In the case of magnesium deposition on the surface of $\beta\sqrt{3}$-Bi at room temperature, LEED observations showed the pattern of 2×2 (Figure 1,*f*) in case of coating with Mg > 0.8 ML. This pattern is the same as for the case of magnesium deposition on the surface of $\alpha\sqrt{3}$-Bi, except that a stronger background is observed on the diffractometer screen. As the metal coating increases, the LEED reconstruction pattern 2×2 blurs and gradually disappears after deposition of > 2 ML of magnesium (Figure 1,*g*), leaving only diffuse reflections from the Si(111)1×1 surface in the diffraction pattern.

For comparison, magnesium was deposited on an atomically pure Si(111)7×7 surface. At the initial stage of deposition, a diffuse LEED pattern 7×7 is observed, confirming the disordered structure of the magnesium film. With a further increase in the magnesium coating to ∼ 8 ML, the LEED pattern corresponds to the crystal structure of the Mg(0001)1×1 film. It is known that the growth of magnesium films on the surface of Si(111) includes several stages [18]: a film of amorphous silicide Mg_2Si is formed on the surface of the substrate at the initial stage, and first a disordered magnesium layer grows on top of it, and upon further deposition, the magnesium film forms a volume-like lattice of Mg(0001), which is observed in our case.

Figure 2,*a, b* shows the STM images of the surface phase of Si(111)2×2-(Bi,Mg) formed by precipitation of magnesium onto the surface of $\alpha\sqrt{3}$-Bi at room temperature. The 2×2 phase exhibits a characteristic cellular structure visible in both images (empty and filled states). A more detailed inspection shows that the surface contains a large number of defects, such as domain boundaries, small clusters (visible as bright spots), and islands, which may be due to the fact that the original surface of $\alpha\sqrt{3}$-Bi itself contains a large number of defects due to competing the process of replacing bismuth atoms with silicon atoms, and part of the magnesium atoms arriving on the surface interact with silicon atoms on the surface.

Another interesting feature is the observation in the LEED of the periodicity 2×2, rotated by 15° after deposition of 2.7 ML of magnesium on the surface of $\alpha\sqrt{3}$-Bi (see Figure 1,*d*), which is not observed after sputtering of magnesium onto $\beta\sqrt{3}$-Bi surface. However, observations using the STM method show that in the latter case, large islands of faceted shape are visible on the surface. Figure 2,*c* shows an STM image of a typical island with a flat top, which shows an area with the structure 2×2. It can be seen that this structure is misoriented relative to the main crystallographic directions of the Si(111) substrate at an angle of ∼ 15°, which confirms the features of the LEED pattern in Figure 1,*d*. However, due to the fact that the island area occupies < 5% of the surface area of the substrate, the LEED method in the case of a surface with magnesium adsorbed onto the $\beta\sqrt{3}$-Bi phase displays a picture only of the disordered silicon surface. It can be concluded that the grown magnesium film contains a structure 2×2-15°, which is not visible for the Mg-coated substrate of $\beta\sqrt{3}$-Bi due to the too small surface area

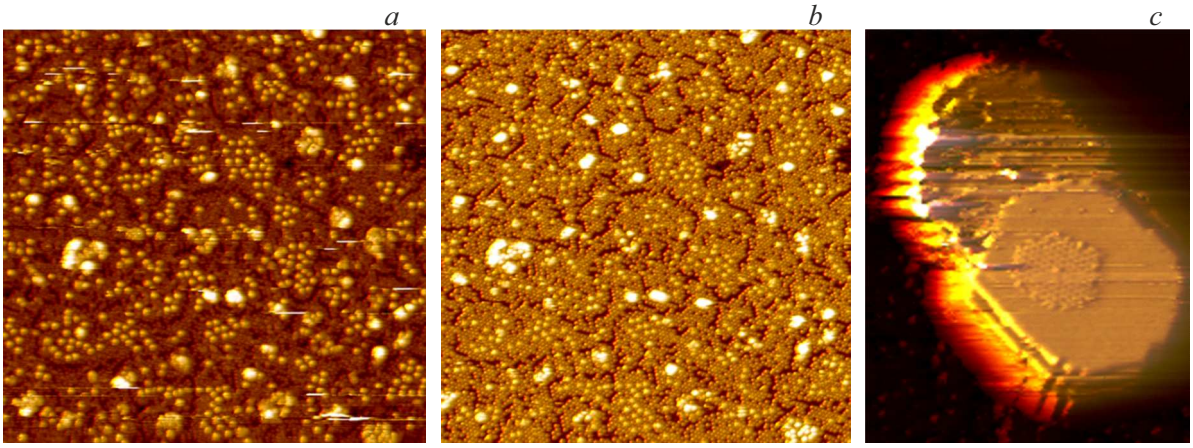

Figure 2. STM patterns (86×84 nm) of surface reconstruction of Si(111)2×2-(Bi,Mg) obtained by adsorption of 1.3 ML of magnesium onto the surface of $\alpha\sqrt{3}$-Bi at room temperature: *a* — $V_s = +1.4$ V (empty states) and *b* — $V_s = -1.4$ in (filled states). *c* — picture of the STM (50×50 nm) island with the structure of 2×2-15° on the vertex plane.

of the Mg islands on this surface, but appears in the diffraction pattern for the Mg-coated substrate of $\alpha\sqrt{3}$-Bi. On the other hand, a structure with a periodicity 2×2 has never been observed on the surface of magnesium films, which means that this periodicity can be concluded that this periodicity is the result of the formation of a joint structure of bismuth and magnesium. As previously found in Refs. [10,14], the difference in the growth regime of the deposited film on samples of $\alpha\sqrt{3}$-Bi and $\beta\sqrt{3}$-Bi can be explained by the different chemical activity of these surfaces. While the surface of $\alpha\sqrt{3}$-Bi contains unsaturated dangling bonds caused by substituting Si atoms, the surface of $\beta\sqrt{3}$-Bi is chemically more inert, and, consequently, the adsorbed magnesium atoms on such a surface have high mobility. In the first case, the surface has a large number of defects on which the adsorbed magnesium atoms interact with the silicon atoms of the substrate and form a large number of nucleation centers, which coalesce to form a continuous film, whereas in the second case, in the surface phase $\beta\sqrt{3}$-Bi, the bismuth layer is denser and almost It is defect-free, therefore, the adsorbed magnesium atoms have a sufficiently long diffusion length over the surface and assemble into isolated islands separated from each other. A joint analysis of the LEED and STM patterns confirms this behavior for the case of adsorption of other elements, for example, gold on Bi-passivated surfaces of Si(111) [10].

The tendency to form joint ordered structures on Si(111) with the participation of bismuth and magnesium is also observed on the sample surface and in cases where both the concentration of both elements and the temperature of the substrate are changed. The surface structure was studied using LEED and STM methods on a Si(111) substrate coated with both $\alpha\sqrt{3}$-Bi and $\beta\sqrt{3}$-Bi phases together (the total Bi coating is $\sim 0.5-0.6$ ML). This allows us to observe how magnesium atoms interact with bismuth-coated areas of the surface with different chemical activity. Thus, it was found that if the initial surface consists of a mixture of $\alpha\sqrt{3}$-Bi and $\beta\sqrt{3}$-Bi structures, the temperature of the substrate during magnesium deposition affects the evolution of the surface structure. Initially, as in previous cases, deposition of > 0.8 ML of magnesium onto this surface during RT leads to the appearance of a LEED pattern 2×2, however, annealing of the resulting surface at a temperature of > 100 °C contributes to the formation of an ordered structure $\sqrt{7}\times\sqrt{3}$ (Figure 3, *a, b*). Further annealing at 200 °C leads to the formation of an ordered structure $c(2\sqrt{3}\times4)$ (Figure 3, *c, d*), which transforms into the structure 2×4 (Figure 3, *e*) after subsequent deposition of $0.1-0.3$ ML of Mg at $c(2\sqrt{3}\times4)$ at room temperature. In the case of annealing slightly higher than 200 °C, a reconstruction of the surface with the structure 5×5 is observed (Figure 3, *f*). Heating of the substrate at 300 °C leads to repeated restoration of the surface with phase $\alpha\sqrt{3}$-Bi due to magnesium desorption at this temperature. Thus, the substrate temperature increases from 100 to 300 °C leads to the formation of joint structures of magnesium and bismuth with different frequency: $\sqrt{7}\times\sqrt{3}$, $c(2\sqrt{3}\times4)$, 2×4 and 5×5. Such a variety of surface structures makes it possible to fairly accurately calibrate the concentrations of elements (bismuth and magnesium) on the surface of Si(111), as well as adjust the temperature regime of the substrate. However, it can be noted that all these two-dimensional structures have a weak effect on the electrical conductivity of the samples. Thus, the electrical resistance of substrates with reconstructions of (Bi,Mg)/Si(111): 2×2, $\sqrt{7}\times\sqrt{3}$, $c(2\sqrt{3}\times4)$, 2×4 and 5×5 remain approximately the same as the electrical resistance for the initial substrate with surface phase Si(111)$\sqrt{3}\times\sqrt{3}$-Bi, which is related to the semiconductor nature of the electronic structure of these surfaces. So, in Figure 4, *a* and *b* represent STM patterns from surface reconstructions of Si(111)$\sqrt{7}\times\sqrt{3}$-(Bi,Mg) and Si(111)$c(2\sqrt{3}\times4)$-(Bi,Mg), which demonstrate good surface ordering for these samples, and in Figure 4, *c* the spectrum of scanning tunneling spectroscopy (STS) for the

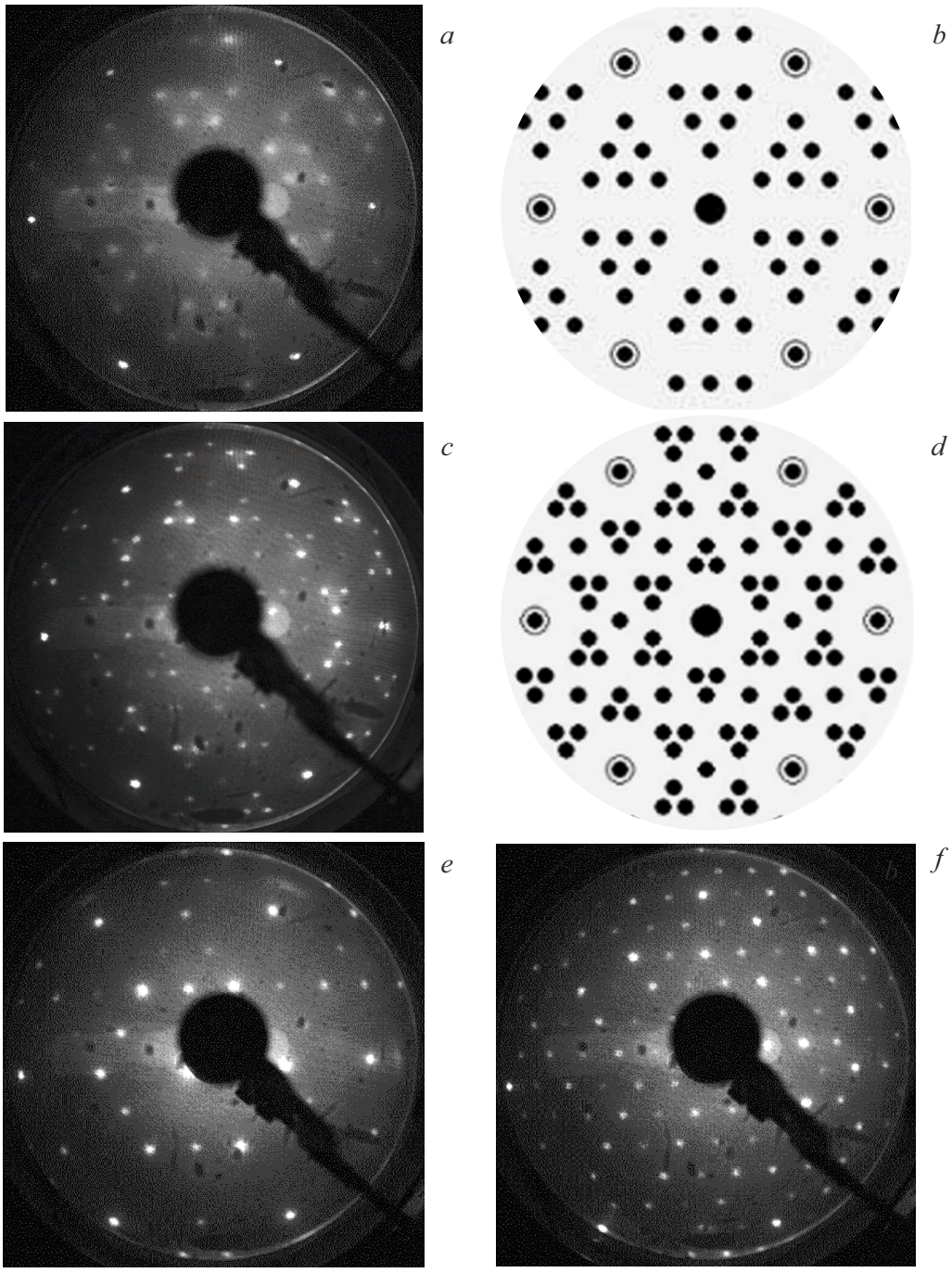

Figure 3. LEED patterns ($E_p = 40$ eV) for structures (Mg,Bi)/Si(111): *a* — structure $\sqrt{7}\times\sqrt{3}$ and *b* — its schematic representation, *c* — structure $c2\sqrt{3}\times4$ and *d* — its schematic representation, *e* — LEED painting 2×4, *f* — LEED painting 5×5. The schematic images were constructed using the LEEDpat program [19].

surface of Si(111)$\sqrt{7}\times\sqrt{3}$-(Bi,Mg) is presented and the spectrum of the STS surface $\alpha\sqrt{3}$-Bi is presented for comparison. It can be seen that the spectra contain an energy gap (band gap) of ~ 0.9 and $0.5-0.6$ eV for surfaces $\sqrt{7}\times\sqrt{3}$-(Bi,Mg) and $\alpha\sqrt{3}$-Bi, respectively.

At the same time, changes in the surface morphology of magnesium films on a Bi/Si(111) substrate they are well manifested in their electrical properties. Four tungsten probes were lowered onto the sample surface immediately after magnesium deposition at room temperature for *in situ* measurements of the electrical resistance of the substrates. Figure 5 shows the results of measurements of the electrical resistance of magnesium films grown on $\alpha\sqrt{3}$-Bi or $\beta\sqrt{3}$-Bi surfaces, as well as on various reconstructions of surface (Mg,Bi)/Si(111), including $\sqrt{7}\times\sqrt{3}$, $c(2\sqrt{3}\times4)$, and on the surface of Si(111)7×7, given for comparison. It can

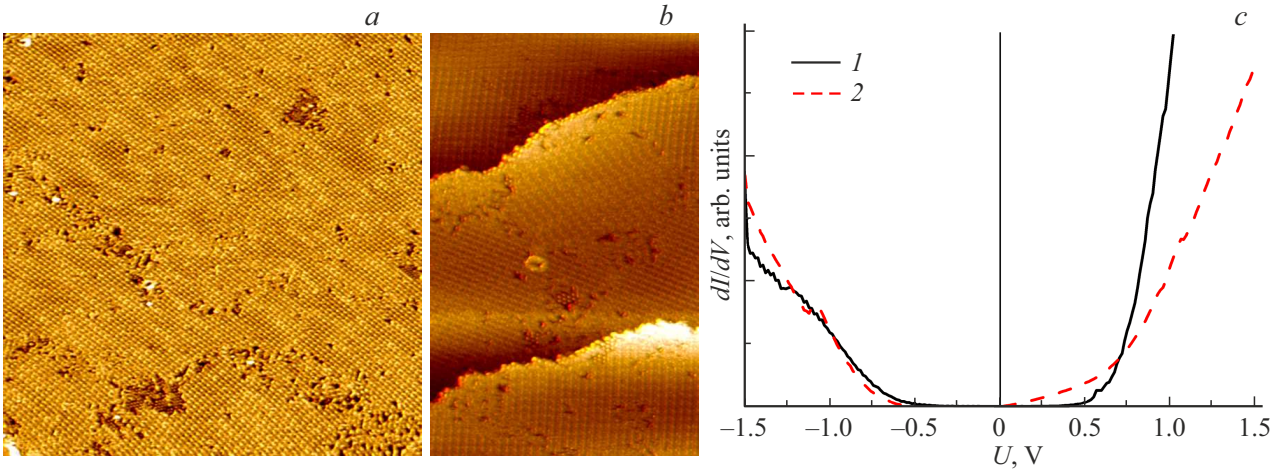

Figure 4. *a* — STM surface reconstruction patterns Si(111)$\sqrt{7}\times\sqrt{3}$-(Bi,Mg) (100×100 nm, $V_s = -1.4$ V, $I = 0.8$ nA) and *b* — surface reconstruction of Si(111)$2\sqrt{3}\times4$-(Bi,Mg) (100×50 nm, $V_s = -1.5$ V, $I = 0.8$ nA), *c* — STS spectrum for surfaces $\beta\sqrt{3}$-Bi and $\sqrt{7}\times\sqrt{3}$-Bi,Mg (red and black graphs, respectively).

be seen that the initial surfaces are characterized by low conductivity (high resistance), and depending on the initial surface structure, the resistance of the sample exhibits different behavior after magnesium adsorption. So, in the case of sputtering of magnesium onto the surface of $\beta\sqrt{3}$-Bi, the electrical resistance remains almost unchanged, whereas in the case of sputtering of magnesium onto $\alpha\sqrt{3}$-Bi, the resistance of$R$ decreases in close accordance with the dependence of $R \sim 1/\Theta$, where Θ is the coating thickness of the adsorbed material in ML, corresponding to the concentration of adsorbed atoms, which, with an adhesion coefficient close to unity and a layered (or quasi-layered) film growth mechanism, may correspond to the classical law $R \sim 1/d$ for thin films, where d is the thickness of the film. This dependence of the resistance on the amount of adsorbed magnesium indicates that in the first case we are dealing with island growth of an ultrathin film, when the formed film is not continuous, but consists of islands between which there is no electrical contact, which is confirmed by observations of STM patterns. In the second case, a monotonous decrease in electrical resistance with an increase in the amount of adsorbed magnesium indicates that the film grows by a mechanism close to layered growth. It can be noted that the resistance of films at the initial stage of magnesium deposition (coating from 0 to 1−2 ML) does not change, which can be explained by the fact that with this coating, the surface phases formed in this range of coatings have low electrical conductivity (for example, phases $\sqrt{7}\times\sqrt{3}$-(Bi,Mg) and $\alpha\sqrt{3}$-Bi have a semiconductor electronic structure, see Figure 4, *c*), and a solid film of magnesium has not yet formed. However, if the dose of adsorbed magnesium exceeds 3−4 ML, then the resistance of such a film decreases sharply due to layer-by-layer growth. Moreover, this also indicates that the magnesium film is metallic, because the presence of a buffer layer in the form of a $\alpha\sqrt{3}$-Bi phase is an obstacle

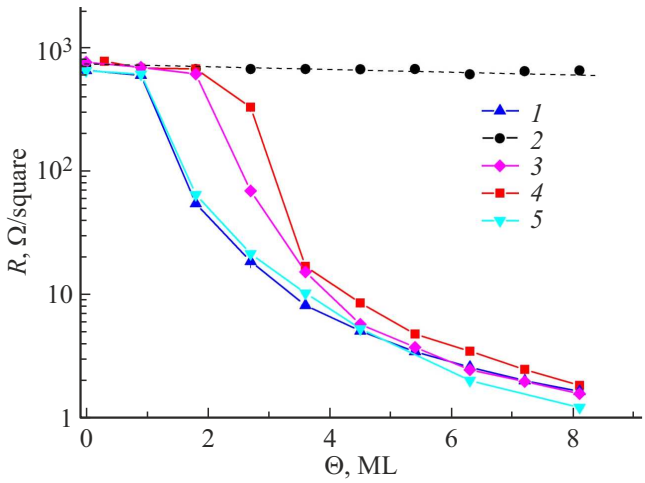

Figure 5. Electrical resistance of silicon samples after deposition of magnesium at room temperature on the substrate surface with reconstructions of $\alpha\sqrt{3}$-Bi (*1*), $\beta\sqrt{3}$-Bi (*2*), $\sqrt{7}\times\sqrt{3}$-(Bi,Mg) (*3*), $c2\sqrt{3}\times4$-(Bi,Mg) (*4*). Changes of the electrical resistance of the sample after sputtering of magnesium onto Si(111)7×7 surface of pure silicon (*5*) are shown for comparison.

to the formation of semiconductor magnesium silicide, and, accordingly, this deposition method allows for the surface of the Si(111) substrate to grow ultrathin layers of metallic magnesium, the electrical conductivity of which can vary depending on its thickness and the coating of bismuth in the buffer layer.

4. Conclusion

A number of experiments were conducted in this work to study the effect of magnesium adsorption on

the crystal structure and electrical resistance of Si(111) silicon substrates with Si(111)$\sqrt{3}\times\sqrt{3}$-Bi reconstructions preformed on their surface. New reconstructions have been discovered in the (Bi,Mg)/Si(111) submonolayer system: 2×2, $\sqrt{7}\times\sqrt{3}$, $c(2\sqrt{3}\times4)$, 2×4 and 5×5, the conditions of their formation are defined. It has been found that the electrical resistance of samples with ultrathin magnesium films depends on how the atoms of the adsorbed magnesium interact with the underlying reconstruction of surface of $\alpha\sqrt{3}$-Bi or $\beta\sqrt{3}$-Bi, which in this case plays the role of a buffer layer and prevents the interaction of magnesium with the atoms of the substrate. It is shown that magnesium films deposited on the reconstructed surface $\alpha\sqrt{3}$-Bi exhibit the lowest electrical resistance, while the resistance of the substrate with the phase $\beta\sqrt{3}$-Bi does not change after magnesium deposition due to the island growth of the film.

Funding

The work was performed under the state assignment of the Ministry of Science and Higher Education of the Russian Federation (FWFW-2021-0002).

Conflict of interest

The authors declare no conflict of interest.

References

[1] N. Spiridis, J. Korecki. Appl. Surf. Sci., **141**, 313 (1999). DOI: 10.1016/S0169-4332(98)00518-2
[2] N. Nagamura, I. Matsuda, N. Miyata, T. Hirahara, S. Hasegawa, T. Uchihashi. Phys. Rev. Lett., **96**, 256801 (2006). DOI: 10.1103/PhysRevLett.96.256801
[3] T. Uchihashi, C. Ohbuchi, S. Tsukamoto, T. Nakayama. Phys. Rev. Lett., **96**, 136104 (2006). DOI: 10.1103/PhysRevLett.96.136104
[4] D.A. Tsukanov, M.V. Ryzhkova, D.V. Gruznev, O.A. Utas, V.G. Kotlyar, A.V. Zotov, A.A. Saranin. Nanotechnology, **19**, 245608 (2008). DOI: 10.1088/0957-4484/19/24/245608
[5] S. Chandola, N. Esser. J. Vac. Sci. Technol. B, **36**, 04H103 (2018). DOI: 10.1116/1.5031228
[6] T. Kuzumaki, T. Shirasawa, S. Mizuno, N. Ueno, H. Tochihara, K. Sakamoto. Surf. Sci., **604**, 1044 (2010). DOI: 10.1016/j.susc.2010.03.022
[7] S. Nakatani, T. Takahashi, Y. Kuwahara, M. Aono. Phys. Rev. B, **52**, R8711 (1995). DOI: 10.1103/PhysRevB.52.R8711
[8] R.H. Miwa, T.M. Schmidt, G.P. Srivastava. J. Phys.: Condens. Matter, **15**, 2441 (2003). DOI: 10.1088/0953-8984/15/17/302
[9] L. Chi, J. Nogami, C.V. Singh. Phys. Rev. B, **103**, 075405 (2021). DOI: 10.1103/PhysRevB.103.075405
[10] D.A. Tsukanov, S.G. Azatyan, M.V. Ryzhkova, E.A. Borisenko, O.A. Utas, A.V. Zotov, A.A. Saranin. Appl. Surf. Sci., **476**, 1 (2019). DOI: 10.1016/j.apsusc.2019.01.063
[11] N.V. Denisov, A.Yu. Tupchaya, A.N. Mihalyuk, L.V. Bondarenko, O.A. Utas, S.G. Azatyan, A.V. Zotov, A.A. Saranin. Surf. Sci., **677**, 291 (2018). DOI: 10.1016/j.susc.2018.08.008
[12] N.V. Denisov, E.N. Chukurov, Yu.V. Luniakov, O.A. Utas, S.G. Azatyan, A.A. Yakovlev, A.V. Zotov, A.A. Saranin. Surf. Sci., **623**, 17 (2014). DOI: 10.1016/j.susc.2014.01.003
[13] A.N. Mihalyuk, L.V. Bondarenko, A.Y. Tupchaya, T.V. Utas, Y.E. Vekovshinin, D.V. Gruznev, S.V. Eremeev, A.V. Zotov, A.A. Saranin. Phys. Rev. B, **104**, 125413 (2021). DOI: 10.1103/PhysRevB.104.125413
[14] M. Naitoh, H. Shimaya, N. Oishi, F. Shoji, S. Nishigaki. Appl. Surf. Sci., **123**, 171 (1998). DOI: 10.1016/S0169-4332(97)00509-6
[15] S. Hasegawa, X. Tong, S. Takeda, N. Sato, T. Nagao. Progr. Surf. Sci., **60**, 89 (1999). DOI: 10.1016/S0079-6816(99)00008-8
[16] A. Saranin, A. Zotov, V. Lifshits, M. Katayama, K. Oura. Surf. Sci., **426**, 298 (1999). DOI: 10.1016/S0039-6028(99)00283-6
[17] A.V. Slyshkin, A.Y. Tupchaya, L.V. Bondarenko, D.V. Gruznev, A.N. Mihalyuk, A.V. Zotov, A.A. Saranin. Thin Sol. Films, **754**, 139317 (2022). DOI: 10.1016/j.tsf.2022.139317
[18] D. Lee, G. Lee, S. Kim, C. Hwang, J.-Y. Koo, H. Lee. J. Phys.: Condens. Matter, **19**, 266004 (2007). DOI: 10.1088/0953-8984/19/26/266004
[19] Fritz Haber Institute of the Max Planck Society, LEEDpat4 software. https://www.fhi.mpg.de/958975/LEEDpat4

Translated by A.Akhtyamov